# Journal of Materials Chemistry A

Accepted Manuscript


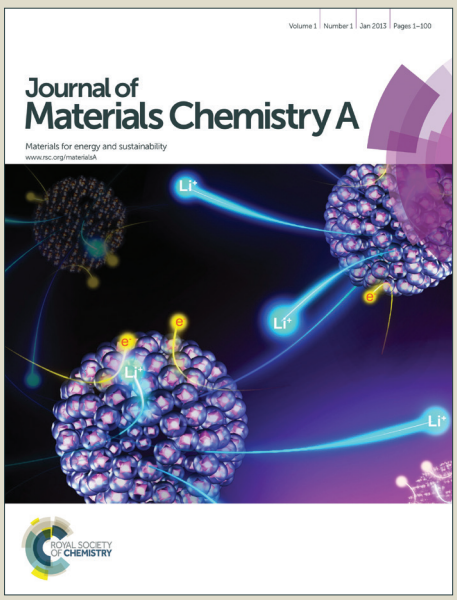





ROYAL SOCIETY OF CHEMISTRY

www.rsc.org/materialsA

Cite this: DOI: 10.1039/c0xx00000x

www.rsc.org/xxxxxx

ARTICLE TYPE

# Tunable electronic and magnetic properties of graphene-like ZnO monolayer upon doping and CO adsorption: a first-principles study

*Yong-Hui Zhang,[a,*] Mei-Ling Zhang,[a] Ye-Cheng Zhou,[b] Ji-Hong Zhao,[a] Shao-Ming Fang,[a] and Feng Li[a,*]*

*Received (in XXX, XXX) Xth XXXXXXXXX 20XX, Accepted Xth XXXXXXXXX 20XX*
**DOI: 10.1039/b000000x**

Graphene-like zinc oxide monolayer (g-ZnO) is a new class of two-dimentional nanomaterials with unique new properties that is still much unknown. This work studies the tunability of the electronic and magnetic properties of g-ZnO upon chemical doping (with B, N and C) and CO adsorption by using first-principles calculations. Both electronic and magnetic properties of g-ZnO exhibit strongly dependency on its structure change and molecular adsorption. The g-ZnO with oxygen atom substituted by a C or N atom (one atom per supercell) are ferromagnetic (FM) half metal (HM), while that substituted by a B atom is a FM semiconductor. The doped g-ZnO shows strong chemisorption to CO molecule by forming A-CO bond (A = B, N or C), in contrast to the weak physisorptionof the intrinsic g-ZnO. Furthermore, CO adsorption converts the N- and C-doped g-ZnO to n-type semiconductor with nonmagnetic (NM) ground states, while B-doped g-ZnO becomes a ferromagnetic half metal (FM-HM). The mechanism for the property change has been investigated by analyzing their partial density of states (PDOS) upon different conditions. This study provides insights to the physical properties and chemical reactivity of g-ZnO, which could help to realize their diverse potentials in electronic and magnetic devices.

## 1 Introduction

Graphene,[1] a single atom layer thick two-dimensional (2D) material, has been extensively investigated in transparent electrodes,[2,3] spintronic devices,[4] composites,[5] gas sensors[6,7] because of its unique structural, mechanical and electronic properties. However, a perfect graphene has almost zero band gap, which prevents it to be used in switching type electronics and many optical applications. In the last few years, new classes of two-dimentional nanomaterials with intrinic band-gap have attracted much interest. Zinc oxide (ZnO), whose band gap 3.37 eV, is one of the mostly studied semiconductor materials, because of its high transparency, piezoelectricity and biocompatibility. ZnO nanostructures have been readily applied in designing chemical sensors, energy storage devices, and transistors.[8,9] ZnO materials with diverse morphologies, such as nanorings,[10] nanosphere,[11,12] nanotubes,[13] nanowires,[14-17] nanobelts,[18] nanosheets,[19] nanaoparticles,[20] and nanoclusters[21,22] have already been synthesized successfully for tuning their functionalities.

While it is rare so far, based on first-principles calculation, graphene-like ZnO nanosheets (g-ZnO) could also exist and exhibit unique properties including optical property. The successful synthesis of g-ZnO (similar to a single atomic layer of graphite sheet) in experimental have awakened an enormous interest in this two-dimensional material. Previous theoretical work predicts that the (0110)-oriented ZnO nanowires can undergo a phase transformation from wurtzite, which is most stable form of ZnO at ambient temperature and pressure, to hexagonal structure under uniaxial tensile loading.[23] The g-ZnO of monolayer with graphene-like structure has a direct wide band gap.[24,25] It was found in experiments that planar ZnO sheets of two-layer-thick with hexagonal graphitic structure can be deposited on a Ag (111) surface.[26] Single- and bilayer ZnO has been prepared by reactive deposition of Zn on Au(111) using X-ray photoelectron spectroscopy and STM by Deng *et al*.[27]g The experimental results revealed that very thin films of polar (0001) surface of ZnO show graphene-like structure.[28] Hur *et al*[29] also reported ZnO thin films with graphene-like structure by *in situ* synchrotron x-ray scattering. Recently, it was reported that the electronic structure and magnetic property of g-ZnO could be tuned by introducing dopant, vacancy and adsorption into the system. For example, Schmidt *et al*[30] have investigated the properties of g-ZnO doped with Co, and indicated that the Co doped Zn site suffers a Jahn-Teller distortion. Topsakal and coworkers[25] presented the atomic, electronic, and magnetic properties of single and bilayer ZnO with honeycomb structure. In addition, it was revealed that fully fluorinated ZnO sheet prefers a twist-chair conformation and is a nonmagnetic semiconductor. In contrast, the most stable F-center conformation

[a]*College of Materials and Chemical Engineering, State Laboratory of Surface and Interface Science andTechnology (SLSIST), Collaborative Innovation Center of Environmental Pollution Control and Ecological Restoration, Zhengzhou University of Light Industry, Zhengzhou, 450002, Henan, P. R. China*
*Fax: (+) 86-371-86609676; 86-371-86609676*
*E-mail: yonghuizhang05@gmail.com; lifeng696@yahoo.com*
[b]*School of chemistry, University of Melbourne , Victoria 3010, Australia*

of semifluorinated ZnO sheet exhibits half-metallic behavior.[31] The fluorination of few layered g-ZnO can induce ferromagnets and half metallicity.[32] Furthermore, nonmetal doped ZnO were also investigated in the past years. Sulfur-doped ZnO nanowires,[33] heterostructure based on N-doped ZnO[34] were successfully synthesized in experimental. 2D g-ZnO monolayer with O atoms substituted by C, N, or B atoms can also make the g-ZnO to exhibit a "nonmagnetic- antiferromagnetic-ferromagnetic" transition.[35] It was reported that ZnO nanoribbon's half metal ferromagnetism can be enhanced by using edge passivation with hydrogen, sulfur, $NH_2$, or $CH_3$.[36,37] To date, most of the available theoretical researches on g-ZnO are mainly based on analyzing their band gap and magnetism. While, the property changes of g-ZnO upon interaction with small molecules are rarely studied. The effects of such"dynamic" interactions could be critical when the materials is used in conditions invovling variable chemical enviorments, such like chemical sensing and catalysis.

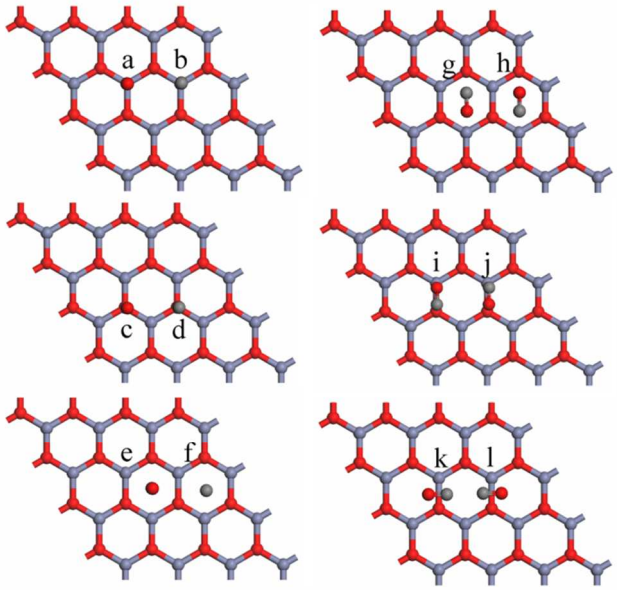


**Fig. 1** Illustration to the twelve available binding sites for CO adsorption on pristine ZnO. The Zn, O and C atoms are shown in pink, blue, grey, and red, respectively.

The researches in our group have concentrated on tuning the functionalities of ZnO materials through controlling their nanostructures. ZnO hexagonal rings and disks were produced on a large scale based on a controlled growth of supercrystals in nanoreactors.[10] Nanoarchitectures including Pd nanoparticles@ZnO nanowires and Pd nanoparticles@ZnO nanosheets have been constructed successfully to fabricate $H_2S$ and acetone sensors with highly improved performances, respectively.[15,38] It was found that the gas sensing functionalities of ZnO materials are closely dependent on their microstructures and surface modifications. Recently, we found that ZnO twin-spheres exposed in highly polar ±(001) facets, which exhibit anisotropic blue emission for the special surface of the particles, can be synthesized successfully with a stepwise self-assembly growth method.[39] Herein, using first-principles calculations, we exploited dopant effects on the functionality of g-ZnO sheet by introducing CO molecule into the system for understanding the gas sensing mechanism of the materials. CO molecule can be used as a probe to study the chemical reactivity of modified g-ZnO sheets. Compared with the very inert surface of pristine g-ZnO sheet, the doped g-ZnO sheets show much higher affinities with CO molecule. Meanwhile, doped g-ZnO sheet-CO systems also exhibit narrowed band gap and interesting magnetic properties. This work may open new pathway for tailoring the functionalities of ZnO nanostructures for making microdevices such as chemical sensors.

## 2 Calculation method and model

All calculations were performed within the framework of spin-polarized plane-wave DFT, implemented in the Vienna ab initio simulation package (VASP).[26, 27] The local density approximation (LDA) for the plane-wave basis set was used in all relaxation process. Each system consisted of a 12.30x12.30x15.00 Å ZnO-sheet super cell (32 atoms) with a single molecule adsorbed in the center region (Fig. 1). The distance between the adjacent g-ZnO layers was kept as 15 Å. An energy cutoff of 500 eV is used for the plane-wave expansion of the electronic wave function. The *k*-point was set to 5x5x1 for the Brillouin zone integration. The structural configurations of the isolated g-ZnO were optimized through fully relaxing the atomic structures. With the same super cell and *k*-point samplings, the configurations of the g-ZnO/molecule systems were optimized through fully relaxing the atomic structures until the remaining forces were smaller than 0.01 eV/Å. The binding energy of CO on g-ZnO was calculated as:

$$E_b = E_{(g\text{-}ZnO/CO)} - E_{(g\text{-}ZnO)} - E_{(CO)}$$

where $E_{(g\text{-}ZnO/CO)}$, $E_{(g\text{-}ZnO)}$ and $E_{(CO)}$ are the total energies of the relaxed g-ZnO/CO system, ZnO and the CO molecule, respectively. In the following section, the non-metal doped g-ZnO are also investigated. Because the radius of B, N, C are close to O, one O atom was replaced by one B, N or C atom for reducing complexity. The percentages of B-, N-, and C- dopant are 0.85wt%, 1.08wt%, 0.93wt% in thedoped g-ZnO system, respectively, based on ZnO-sheet super cell with 32 atoms.Furthermore, test calculation shows that using a higher cut-off energy (700 eV), 8x8x1 k-points or a larger vacuum gap (20 Å) between the g-ZnO sheets made little improvement to the simulation results.

## 3 Results and discussions

In order to verify the accuracy of our calculations, we first perform the calculations on the pristine ZnO sheet and compare our results with previous studies. The initial structure of the ZnO monolayer is cut from a bulk wurtzite ZnO with (0001) polar surface, consistent with the structure of ZnO monolayer synthesized experimentally. The optimized structure of monolayer ZnO sheet is a graphene-like flat plane. The calculated Zn-O bond length is 1.88 Å, which agrees well with the experimental value of 1.92 Å,[26] and previous theoretical values of 1.86 Å by Tu[24] and 1.90 Å by Topsakal et al.[25] Our calculations predict that the ZnO sheet is a NM semiconductor with a LDA

band gap of 1.86 eV, which also agrees well with the previous calculations.

**Table 1.** Binding energy ($E_b$), equilibrium g-ZnO/CO distance ($d$) (defined as the shortest atom-to-atom distance), and Mulliken charge ($Q$) of CO molecule adsorbed on different g-ZnO sheet.

| System | *E*ad (eV) | *d* (Å) | *Q*(*e*)[a] |
|---|---|---|---|
| a | -0.035 | 2.48 | 0.05 |
| b | -0.019 | 2.49 | 0.03 |
| c | -0.33 | 2.67 | 0 |
| d | -0.012 | 2.76 | 0.02 |
| e | -0.17 | 2.67 | -0.06 |
| f | -0.040 | 2.78 | 0.01 |
| g | -0.19 | 2.79 | 0 |
| h | -0.35 | 2.23 | -0.05 |
| i | -0.0054 | 3.30 | 0 |
| j | -0.012 | 3.21 | 0 |
| k | -0.32 | 3.19 | 0 |
| l | -0.27 | 3.31 | 0 |
| B-g-ZnO/CO | -4.05 | 1.43 | -0.24 |
| N-g-ZnO/CO | -2.77 | 1.24 | -0.04 |
| C- g-ZnO/CO | -5.65 | 1.32 | -0.16 |

[a]$Q$ is defined as the total Mulliken charge on the molecules, and negative number means charge transfer from g-ZnO to molecule.

To understand the optimal binding configuration of CO molecule on the pristine g-ZnO, twelve different adsorption configurations were studied (Fig. 1). Different adsorption sites with CO oriented perpendicular to the g-ZnO sheet were considered, including atop a zinc atom, at the center of the hexagon, atop an oxygen atom. For each site, two orientations of the CO molecule were considered, with either C (referred as the CO configuration) or O (referred as the OC configuration) close to the sheet surface. Several other configurations with the CO molecule placed parallel to the hexagonal plan were also tested. Each structure was fully relaxed, and the calculated binding energy, charge transfer, and distance between the adsorbed molecule and the sheet are summarized in Table 1. After full relaxation, the configuration with the CO axis aligned parallel to the hexagonal plan along the diagonal Zn-O direction with the C close to Zn atom (Fig. 1h) was found to be the most stable atomic arrangement. This adsorption configuration gives the highest binding energy ($E_b$ = -0.35 eV) and the shortest distance between CO and g-ZnO ($d$ = 2.67 Å). The calculated binding energy is similar to that of CO adsorbed on carbon nanotubes,[40] boron nitride nanotubes[41] and graphene.[42] The relatively small $E_b$ and large $d$ values indicate that CO undergoes weak physisorption on the pristine g-ZnO, which is consistent with known inert chemical property of g-ZnO materials. The calculated charges of CO adsorbed on g-ZnO from Mulliken population analysis are also provided in Table 1. For the most stable configuration (Fig. 1i), a very small charge (0-0.06 |e|) is transferred from g-ZnO to CO, which indicates their weak interaction.

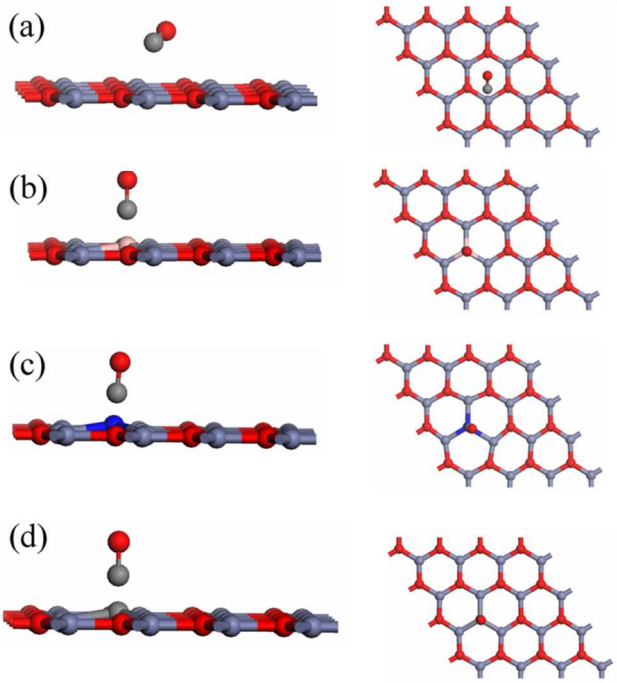


**Fig. 2** Optimized adsorption configurations of CO molecule on g-ZnO (a), the B-g-ZnO (b), N-g-ZnO (c) and C-g-ZnO (d) surface.

When one oxygen atom is substituted by B atom in the super cell, it is found that the geometric structure of the B doped g-ZnO (B-g-ZnO) changes dramatically. Due to the large size of B atom, the B doping results in elongation of the bond length ($l$) at the doping site from $l_{Zn\text{-}O}$=1.876 Å to $l_{Zn\text{-}B}$=2.006 Å. The B atom was pushed away from the plane. This bond length change is associated with the distortion of hexagonal structures adjacent to the B atom, similar to the restructuring in Al doped graphene and carbon nanotubes.[40,42] Like the studies of CO adsorption on the pristine g-ZnO, twelve available adsorption sites have also been evaluated for the CO adsorption on the B-g-ZnO sheet. After relaxation, the configuration in Fig. 2b was found to be the most stable structure, in which the CO molecule is attached to the B site of the B-g-ZnO. In the optimal configuration, the adsorbed CO pulls the B atom out slightly from the sheet plane, leading to a significant change of local geometry of the B-g-ZnO. The formed B-CO bond is titled towards the sheet surface, and the three associated Zn-B-Zn angles are 118.64, 118.33 and 118.25°, respectively. Meanwhile, the three B-Zn bond lengths are changed from 2.006 Å to 2.004, 2.005 and 2.007 Å, respectively, while the length of the B-CO bond is 1.43 Å, indicating that the B site is transformed from $sp^2$ hybridization to more $sp^3$ like hybridization. Moreover, the binding energy of CO on the B-g-ZnO is -4.05 eV, which is over 10 times larger than that of CO on the pristine g-ZnO. The high binding energy and short distance clearly indicate that chemical bond can form during the adsorption process. The binding of CO on the B-g-ZnO is in fact comparable to the binding energies reported in previous investigations on sensors based on doped CNT, such as CO/B-doped CNT (-0.85 eV),[43] suggesting that the B-g-ZnO may be used as a good sensing material for CO.

In the N-doped ZnO (N-g-ZnO) system, the CO molecule was initially placed on the various sites of the N-g-ZnO with different orientations to find the optimal adsorption configurations. The favorable configuration of CO on the N-g-ZnO is similar to the CO on B-g-ZnO systems, i.e. the N atom adopts similar positions like the C atoms in the CO systems. The binding energy is quite exothermic (-2.77 eV), which the C-N length of 1.24 Å. In this case, the charge transfer is -0.04 |e|, indicating an apparent charge transfer from N-g-ZnO to CO. As discussed above, CO cannot be bound to pristine ZnO, but the N-doping makes the para C preferable for CO chemisorption.

When adsorbed in the C-doped g-ZnO (C-g-ZnO), CO molecule prefers to take an orientation with its C atom pointing at the C atom of the C-g-ZnO. The calculation indicates that the dopant provides a stronger binding site for the CO adsorption. The minimum atom to atom distance between the CO and the C-ZnO is 1.32 Å. This distance is in fact close to the bond length of a C-C double bond and is much shorter than that of the pristine ZnO (2.23 Å). The binding energy of CO on the C-g-ZnO can reach -5.65 eV, which is more than one magnitude higher than that of the pristine g-ZnO.

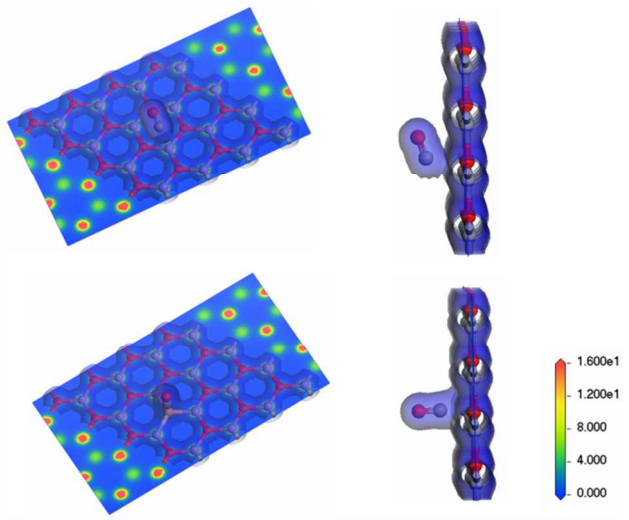


**Fig. 3** Total charge densities of CO interacting with pristine g-ZnO (a) and B-g-ZnO (b).

The electronic total charge density plot for the pristine g-ZnO/CO is compared with that of the CO on the doped-ZnO (take B-g-ZnO for example) in Fig. 3. Little electron orbital overlap between CO molecule and the pristine g-ZnO is observed in Fig. 3a. In contrast, Fig. 3b show that the electronic charge plots of CO and the B-g-ZnO are strongly overlapped, leading to more orbital mixing and larger charge transfer. The total charge density analysis illustrates that only weak physisorption takes place between the CO and pristine g-ZnO, while the dopants provide strong chemisorption binding sites for CO. As the orbital overlap between CO and the B-g-ZnO is much stronger than that of the pristine ZnO is expected to show significant change in its electronic properties upon CO adsorption, therefore is more suitable for sensing applications than the pristine g-ZnO materials.

The electron transfer between CO and the modified g-ZnO sheets were obtained from the Mulliken population analysis (Table 1), which may be qualitatively understood by the fact that the CO adsorption tend to transform the atoms at binding sites from $sp^2$ hybridization to more $sp^3$ like hybridization. As B atoms can only provide three valance electrons, they tend to accept electrons to fill the empty orbitals when transformed to $sp^3$ hybridization. Therefore, charges are transferred from CO to the B-g-ZnO (0.24 |e|). For the doped g-ZnO, large charge transfer occurs between doped g-ZnO and CO molecule. However, little charge is transferred between pristine g-ZnO and CO molecule.

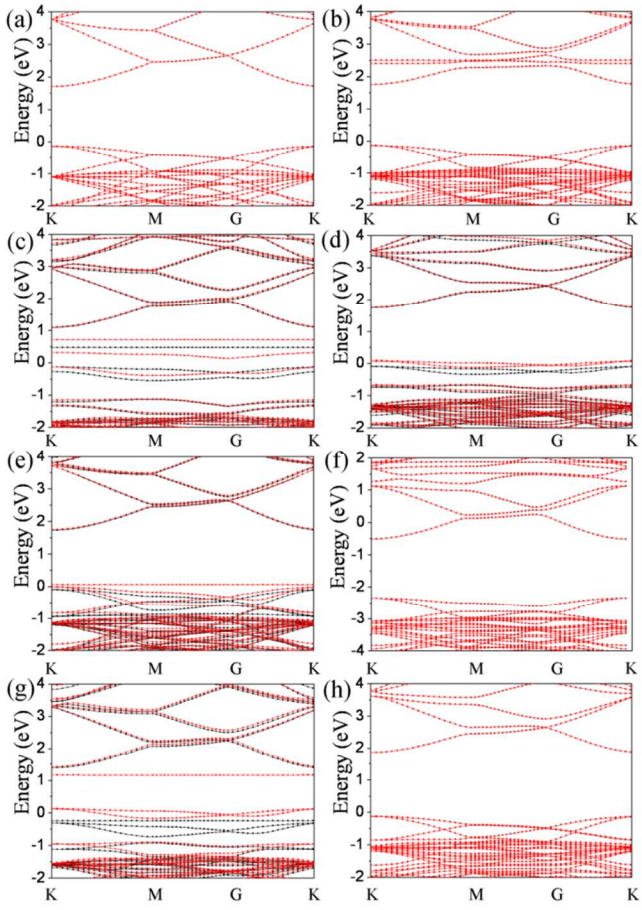


**Fig. 4** The electronic band structure of g-ZnO (a), g-ZnO/CO (b), B-ZnO (c), B-ZnO/CO (d), N-ZnO (e), N-ZnO/CO (f), C-ZnO (g) and C-ZnO/CO (h). The Fermi level is set to zero. The black and red lines represent spin-up and spin-down channels, respectively.

The electronic and magnetic properties of the g-ZnO/CO systems are analyzed from their spin band structure spectra. The calculated majority and minority band for the (a) pristine g-ZnO/CO, (b) C-g-ZnO/CO, (c) B-g-ZnO/CO and (d) N-g-ZnO/CO are shown in Fig. 4. The band structure of the pristine g-ZnO shows a band gap of 1.68 eV (Fig. 4a), indicating an extremely low conductivity. The band structure of g-ZnO/CO shows a small new band at 2.5 eV, while there is no significant change near the Fermi level and the band gap is still large 1.68 eV (Fig. 4b). The contribution of the CO electronic levels to the total band for both systems is localized between -1.0 and -2.2 eV in the valence bands and around 2.5 eV in the conduction bands, which are far away from the Femi level. It indicates little conductivity change upon CO adsorption. The spin up and spin

down channels are identical in Fig. 4a and b, indicating no magnetic moment exists for the pristine g-ZnO either before or after the CO adsorption. Therefore, the pristine g-ZnO is unlikely to serve as electronic sensor for CO molecule.

Next, we consider the B-g-ZnO monolayer with one oxygen atom substituted by a carbon atom per supercell ($Zn_{16}O_{15}B$), as shown in Fig. 2c. The calculated band structure indicates that the B-g-ZnO monolayer is a ferromagnetic (FM) semiconductor with spin-polarized bands apart from the Fermi level (Fig. 4c). The total magnetic moment per supercell of $Zn_{16}O_{15}B$ is 1.02 $\mu_B$. Compared with pristine g-ZnO, the B-g-ZnO configuration presents asymmetrical spin up and spin down bands, which means that the spin degeneracy has been broken. Moreover, one spin-polarized band below the Fermi level and two spin-polarized bands above the Fermi level appear in the spin down channel. Then, one spin-polarized band above the Fermi level appears in the spin up channel. Each spin channel shows semiconducting characteristics; the band gaps are 0.44 and 0.61 eV for spin down and spin-up channels, respectively, which are lower than pristine g-ZnO. B doping also brings impurity states in both spin up and spin down channels below or above the Fermi level. Note that the impurity states in two spin bands are also degenerate. After the introduction of CO into B-g-ZnO surface, the energy bands near the Fermi level become asymmetric for different spin channels: in the spin down channel, the Fermi level is shifted into the conduction band and metallicity is thus obtained, while the spin up is semiconducting with a 1.82 eV gap. Therefore, the B-g-ZnO/CO is HM. The magnetic moment occurs in the B-g-ZnO/CO (0.94 $\mu_B$), which is close to the B-g-ZnO system. After CO adsorption on B-g-ZnO surface, it almost keeps the FM. Similarly, N-g-ZnO containing one N atom doping is also HM, with a metallic spin down channel and a 1.85 eV gap for spin up channel. The introduction of N atom gives many impurity states in valence bands, while the dopant only leads one spin down channel near 0.08 eV above the Fermi level. From Fig. 4e, it can be seen that the spin down channel exceeds the spin up channel by the occupied peak just above the Fermi level and spin up channels shows new bands below the Fermi level between -0.10 eV and -0.95 eV, indicating that magnetic moment occurs in the N-g-ZnO (0.98 $\mu_B$) systems. After binding with the CO molecule, the spin up channels and spin down channels completely overlap together with a band gap of 1.85 eV, indicating the N-g-ZnO/CO is NM property. From the band structure analysis, NM property can be seen compatible with pristine g-ZnO. It is noticeable that when N dopant is applied, as in case Fig. 4e, a magnetic behaviour is observed through crossing the line at the Fermi energy, after the adsorption of CO molecule (case Fig. 4f), NM property is recovered. This variety of fundamental changes on the important electronic properties of the resulting materials is appropriate for manipulation of such modifications.

For C-g-ZnO, its result is close to the N-g-ZnO. When the C atom was doped into the pristine g-ZnO surface replacing with the O atom, the energy bands near the Fermi level become asymmetric for different spin channels, indicating that C-g-ZnO monolayer is a FM materials. It also shows HM property with spin down channels crossing the Fermi level and a 1.61 eV gap for spin up channels. The total magnetic moment per supercell of $Zn_{16}O_{15}C$ is 2.09$\mu_B$, which is consistent with previous report [35]. After adsorption the CO molecule, the C-g-ZnO appear nonmagnetic with a 1.98 eV gap for spin up and spin down channel. The phenomena also confirms that CO can quench the magnetism of C-ZnO.

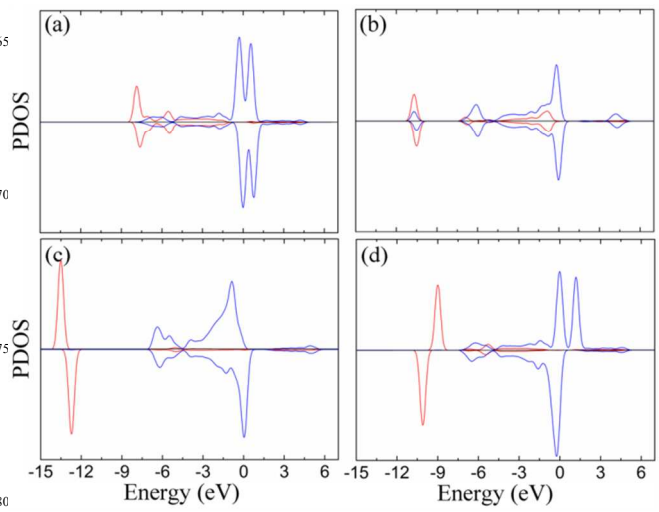


**Fig. 5** The calculated majority and minority DOS of (a) B in B-g-ZnO, (b) B in CO/B-g-ZnO, (c) N in N-g-ZnO, and (d) C in C-g-ZnO. The s and p orbitals are shown in red and blue, respectively. The zero corresponds to the Fermi energy.

The above calculations have revealed that different dopants could tune the nonmagnetic ZnO to magnetic one, while the CO/dopant/ZnO also show different spin polarized properties. To further understand the origins of such different magnetic properties of the doped-ZnO and CO/dopant/graphene systems, the calculated majority and minority DOSs for the (a) B in B-g-ZnO, (b) B in CO/B-g-ZnO, (c) N in N-g-ZnO and (d) C in C-g-ZnO are shown in Fig. 5. The 1*s* and 2*p* orbitals of B in B-g-ZnO contribute to the states near -4.9--8.5 eV, -1.0-1.26 eV. The 1*s* orbitals is far away the Fermi level, while the 2*p* orbitals is near the Fermi level, indicating the mostly contributed magnetic moment of B-g-ZnO coming from the 2p orbitals. Two kinds of unsymmetrical peaks of 2p orbitals in B-g-ZnO appear bellow the Fermi level (-0.28 eV, 0 eV) and above the Fermi level (0.55 eV, 0.79 eV), which induces enhanced magnetic moment. After CO molecule adsorption on B-g-ZnO (Fig. 5b), one kind of unsymmetrical peak of 2p orbitals in B (CO/B-g-ZnO) above the Fermi level disappear, and intensity of another kind bellow the Fermi level also weaken. It indicates the magnetic moment of B in B-g-ZnO (1.09 $\mu_B$) is larger than that of B in CO/B-g-ZnO (0.89$\mu_B$). Although the spin polarized propertie of s orbitals is prominent for B in CO/B-g-ZnO compared to B in B-g-ZnO between -1.56 eV and -0.25 eV, the magnetic properties of B in B-g-ZnO is stronger than B in CO/B-g-ZnO for p orbitals mainly contributed to the spin properties near the Fermi level. For the PDOS of N-g-ZnO and C-g-ZnO, the majority and minority densities of s orbitals are identical in Fig. 5c and d, indicating no magnetic moment exists for the s orbitals either in N-g-ZnO or C-g-ZnO. The local magnetic moment of N-g-ZnO and C-g-ZnO is mainly contributed by the N's 2p orbital and C's 2p orbitals. The spin DOS of the 2p orbitals C-g-ZnO has two remarkable peaks

above the Fermi level (0 eV and 1.18 eV) and one peak below the Fermi level (-0.25 eV), while N-g-ZnO has one peak above the Fermi level (0.04 eV), and one peak below the Fermi level (-0.86 eV). It indicates that the C'2p orbital have higher asymmetry and intensity than N'2p orbital, which also confirms C dopant could induce larger magnetic moment than that of N dopant. The observations of both enhanced electronic and magnetic properties of the g-ZnO through introduction of dopant shall help to establish appropriate methods for chemical modification of the originally inert g-ZnO and to facilitate the applications of this new nanomaterial in the fields of electronic and magnetic devices.

## 4 Conclusions

In summary, the adsorption of CO molecule on the pristine, B-, N- and C-g-ZnO are investigated using DFT calculation. It is found that the CO molecule shows strong interactions with B- and N-g-ZnO, and it even forms chemical bond with the C-g-ZnO. The significantly increased binding energies and charge transfers of CO on the modified g-ZnO are expected to induce significant changes in the electrical conductivity of g-ZnO, and therefore are promising for electronic applications, such as gas sensor. Furthermore, the doped-ZnO shows spontaneous magnetization and changeable magnetism upon CO adsorption, which may be used in sensor or novel magnetic devices.

## Acknowledgements

The authors are grateful to the financial support from the National Natural Science Foundation of China (NSFC. 21301158, 21141005, 21071130 and 21371157), Outstanding Scholar Program of Henan Province (114200510012), Key Program of Henan Province for Science and Technology (132102210424), the School Doctor Foundation of Zhengzhou University of Light Industry (Grant No. 2010BSJJ014), Backbone Teacher Project (2012XGGJS04), Jinshui district for Science and Technology ([23]-17) and the Education Department of Henan Province (No. 12B150030).

1 K. S. Novoselov, A. K. Geim, S. V. Morozov, D. Jiang, Y. Zhang, S. V. Dubonos, I. V. Grigorieva and A. A. Firsov, *Science* 2004, **306**, 666.

2 X. Wang, L. Zhi and K. Mullen, *Nano Lett.* 2009, **8**, 323.

3 H. A. Becerill, J. Mao, Z. Liu, R. M. Stoltenberg, Z. Bao and Y. Chen, *ACS Nano* 2008, **2**, 463.

4 N. Tombros, C. Jozsa, M. Popinciuc, H. T. Jonkman and B. J. v. Wees, *Nature* 2007, **448**, 571.

5 S. Stankovich, D. A. Dikin, G. H. B. Dommett, K. M. Kohlhaas, E. J. Zimney, E. A. Stach, R. D. Piner, S. T. Nguyen and R. S. Ruoff, *Nature* 2006, **442**, 282.

6 F. Schedin, A. K. Geim, S. V. Moeozov, E. W. Hill, P. Blake, M. I. Katsnelson and K. S. Novoselov, *Nat. Mater.* 2007, **6**, 652.

7 I. I. Barbolina, K. S. Novoselov, M. S. V, S. V. Dubonos, M. Missous, A. O. Volkov, D. A. Christian, I. V. Grigorieva and A. K. Geim, *Appl. Phys. Lett.* 2006, **88**, 013901.

8 D. C. Look, *Mater. Sci. Eng. B* 2001, **80**, 383.

9 Ü. Özgür, Y. I. Alivov, C. Liu, A. Teke, M. A. Reshchikov, S. Doğan, V. Avrutin, S.-J. Cho and H. Morkoç, *J. Appl. Phys.* 2005, **98**, 041301.

10 F. Li, Y. Ding, P. Gao, X. Xin and Z. L. Wang, *Angew. Chem. Int. Ed.* 2004, **43**, 5238.

11 M.-H. Junga, H.-G. Yuna, S. Kimb and M. G. Kang, *Electrochim. Acta* 2010, **55**, 6563.

12 H. Wang, A. Pyatenko, N. Koshizaki, H. Moehwald and D. Shchukin, *ACS Appl. Mater. Interfaces* 2014, **6**, 2241.

13 J. Duan, X. Huang and E. Wang, *Mater. Lett.* 2006, **60**, 1918.

14 G. S. Wu, T. Xie, X. Y. Yuan, Y. Li, L. Yang, Y. H. Xiao and L. D. Zhang, *Solid State Commun.* 2005, **134**, 485.

15 Y. Zhang, Q. Xiang, J. Xu, P. Xu, Q. Pan and F. Li, *J. Mater. Chem.* 2009, **19**, 4701.

16 N. Kumar, A. K. Srivastava, R. Nath, B. K. Gupta and G. D. Varma, *Dalton Trans.* 2014, **43**, 5713.

17 D. Jang, J. Yoon, D. Kim, Y. S. Moon, K. H. Kim and J. S. Ha, *J. Mater. Chem. C* 2013, **1**, 7191.

18 Y. Huang, J. He, Y. Zhang, Y. Dai, Y. Gu, S. Wang and C. Zou, *J. Mater. Sci.* 2006, **41**, 3057.

19 Y. Wang, X. Fan and J. Sun, *Mater. Lett.* 2009, **63**, 350.

20 R. Gao, Y. Cui, X. Liu, L. Wang and G. Cao, *J. Mater. Chem. A* 2014, **2**, 4765.

21 H. Cao, J. Y. Xu, D. Z. Zhang, S. H. Chang, S. T. Ho, E. W. Seeling, X. Liu and R. P. H. Chang, *Phys. Rev. Lett.* 2000, **84**, 5584.

22 S. Zhang, Y. Zhang, S. Huang, H. Liu, P. Wang and H. Tian, *J. Mater. Chem.* 2011, **21**, 16905.

23 A. J. Kulkarni, M. Zhou, K. Sarasamak and S. Limpijumnong, *Phys. Rev. Lett.* 2006, **97**, 105502.

24 Z.C.Tu, *J. Comput. Theor. Nanosci.* 2010, **7**, 1182.

25 M. Topsakal, S. Cahangirov, E. Bekaroglu and S. Ciraci, *Phys. Rev. B* 2009, **80**, 235119.

26 C. Tusche, H. L. Meyerheim and J. Kirschner, *Phys. Rev. Lett.* 2007, **99**, 026102.

27 X. Deng, K. Yao, K. Sun, W.-X. Li, J. Lee and C. Matranga, *J. Phys. Chem. C* 2013, **117**, 11211.

28 F. Claeyssens, C. L. Freeman, N. L. Allan, Y. Sun, M. N. R. Ashfolda and J. H. Harding, *J. Mater. Chem.* 2005, **15**, 139.

29 T.-B. Hur, Y.-H. Hwang, H.-K. Kima and H.-L. Park, *J. Appl. Phys.* 2004, **96**, 1740.

30 T. M. Schmidt, R. H. Miwa and A. Fazzio, *Phys. Rev. B* 2010, **81**, 195413.

31 Y. Wang, Y. Ding, J. Ni, S. Shi, C. Li and J. Shi, *Appl. Phys. Lett.* 2010, **96**, 213117.

32 Q. Chen, J. Wang, L. Zhu, S. Wang and F. Ding, *J. Chem. Phys.* 2010, **132**, 204703.

33 S. Y. Bae, H. W. Seo and J. Park, *J. Phys. Chem. B* 2004, **108**, 5206.

34 H. Qin, W. Li, Y. Xia and T. He, *ACS Appl. Mater. Interfaces* 2011, **3**, 3152.

35 H. Guo, Y. Zhao, N. Lu, E. Kan, X. C. Zeng, X. Wu and J. Yang, *J. Phys. Chem. C* 2012, **116**, 11336.

36 A. R. Botello-Méndez, F. López-Urías, M. Terrones and H. Terrones, *Nano Lett.* 2008, **8**, 1562.

37 A. R. Botello-Méndez, F. López-Urías, M. Terrones and H. Terrones, *Nano Res.* 2008, **1**, 420.

38 Y. Xiao, L. Lu, A. Zhang, Y. Zhang, L. Sun, L. Huo and F. Li, *ACS Appl. Mater. Interfaces* 2012, **4**, 3797.
39 F. Li, F. Gong, Y. Xiao, A. Zhang, J. Zhao, S. Fang and D. Jia, *ACS Nano* 2013, **7**, 10482.
40 R. Wang, D. Zhang, W. Sun, Z. Han and C. Liu, *J. Mol. Struc-THEOCHEM* 2007, **806**, 93.
41 R. J. Baierlea, T. M. Schmidtb and A. Fazzioc, *Solid State Commun.* 2007, **142**, 49.
42 Z. M. Ao, J. Yang, S. Li and Q. Jiang, *Chem. Phys. Lett.* 2008, **461**, 276.
43 S. Peng and K. Cho, *Nano Lett.* 2003, **3**, 513.